Heliyon 10 (2024) e37797

Contents lists available at ScienceDirect

Heliyon

journal homepage: www.cell.com/heliyon

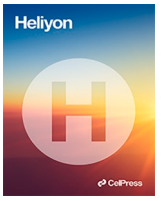

Research article

Plant extract-mediated biosynthesis of sulphur nanoparticles and their antibacterial and plant growth-promoting activity

Khushboo Dasauni [a], Tapan K. Nailwal [a,*], Bhavani Prasad Naik Nenavathu [b]

[a] Department of Biotechnology, Sir J.C. Bose Technical Campus, Bhimtal-263136, Kumaun University Nainital, Uttarakhand-India
[b] Department of Applied Sciences and Humanities, Indira Gandhi Delhi Technical University for Women, Delhi-110006-India

ARTICLE INFO

Keywords:
Sulphur nanoparticles
Cannabis sativa
Antibacterial activity
Pot experiments
Green synthesis

ABSTRACT

This study reports green synthesis of sulphur nanoparticles using sodium thiosulfate pentahydrate ($Na_2S_2O_35H_2O$) and *Cannabis sativa* leaf extracts. X-ray diffraction (XRD) pattern and scanning electron microscopy (SEM) was employed to examine the crystallinity of the particles and morphological characteristics, proved both spherical and rod-shaped morphology of the S NPs having porous nature. The FTIR spectra revealed the interaction of the synthesized SNPs with the biomolecules present in the leaf extract. UV–VIS spectral investigations confirmed the production of SNPs from *C. sativa* leaf extract and that these SNPs can be used for visible region photocatalysis for the removal of pollutants from wastewater. Energy dispersive X-ray (EDX) spectrum of the SNP shows a single peak around 2.4 keV, confirmed S NPs purity. TEM image revealed the formation of mainly nanorods having a width of ~20–25 nm and a length of 50–100 nm. Furthermore, some spherical particles (~20–30 nm) were also formed. HRTEM image of the rod-shaped particles clearly shows the crystal fringe spacing of 0.38 nm. Further, disc diffusion method (DDM) was used to check the antibacterial activity of S NPs against gram-positive *S. aureus* (MTCC737) 18 ± 0.12 mm and gram-negative bacteria against *E. coli* (MTCC443) 21.5 ± 0.12 mm, *A. salmonicida* (MTCC1522) 19.1 ± 0.12 mm, *K. pneumoniae* (MTCC3384) 17.8 ± 0.10 mm. Among all the strains of bacteria, *E. coli* (MTCC443) showed a maximum zone of inhibition of 21.5 ± 0.12 mm and its antibacterial activity is somewhat like streptomycin sulfate. These SNPs also promote growth of *C. sativa* in pot experiment, resulting in a 30 % increase in biomass, 90 cm in shoot length and 28 cm in root length and higher fresh and dry weight (50g and 20g, respectively) with 1.0 mg mL^{-1} NPs treatment. In addition, SEM-EDX confirmed the accumulation of nanomaterial in plant leaves. This environmentally friendly approach to SNP synthesis using *C. sativa* extracts demonstrates both potent antibacterial properties and plant growth-promoting effects, making it a promising solution for agriculture and biomedicine.

1. Introduction

Major advancement has been obtained in the synthesis of nanoparticles, with a special focus on "green synthesis" techniques that are sustainable and economical. This method has drawn a lot of attention because of its ease of use, fast reaction time, and cost efficiency, making it a possible technology for producing clean, biocompatible, and non-toxic nanoparticles. Plant extracts have a remarkable ability to effortlessly create highly ordered hierarchical structures thus, bioinspired approaches have become an effective

* Corresponding author.
E-mail address: drtapannailwal@kunainital.ac.in (T.K. Nailwal).

https://doi.org/10.1016/j.heliyon.2024.e37797
Received 9 December 2023; Received in revised form 21 August 2024; Accepted 10 September 2024
Available online 11 September 2024

method for creating nanoparticles of varied sizes [1]. Moreover, microorganisms, particularly bacteria and fungi, have been extensively explored for their potential as nanomaterial production platforms, leveraging their capabilities to gather and purify heavy metals using reductase enzymes. *Pseudomonas*, *Visella*, *Bacillus*, *Bhargavaea*, and *Brevibacterium* are just a few of the many bacterial genera that have shown the potential to create silver (Ag) and gold (Au) nanoparticles. A number of other genera, including *Lactobacillus*, *Bacillus*, *Streptomyces*, *Klebsiella*, *Enterobacter*, *Escherichia* etc have been reported to be used for nanoparticle synthesis [2–4]. The fungus *Fusarium oxysporum* was challenged with aqueous ZrF62- anions, resulting in the simple room temperature synthesis of nanocrystalline zirconia to successfully synthesize zirconia nanoparticles [5,6]. Additionally, an environmentally friendly synthesis Ni^{2+} Co-doped silica magnesium zirconium copper nanoceramics was conducted, as well as an analysis of their structural, optical, and magnetic properties, which can be used in various applications for water and wastewater treatments [7] Also, the Nickel magnesium copper zircon silicate nano composite already used in biomedical sector to suppress the food borne disease caused by food borne pathogenic bacteria. Expanding the scope, biomaterials, including plants, have served as bioreactors for the modification of metallic ions into metallic nanoparticles, allowing for the synthesis of nanomaterials through a process known as metal bioaccumulation [8,9]. Many plants have been used for the synthesis of Ag nanoparticles including *Aloe vera*, *Tinospora cordifolia*, *Withania somnifera*, *Citrus sinesis*, and many more [10–13]. For both the production and foliar administration of magnesium nanoparticles to wheat plants, a biosynthetic procedure was developed. Additionally, it was found that the fungus protein *Aspergillus brasiliensis* TFR 23 successfully delivered magnesium nanoparticles with predictable particle sizes (5.9 nm). The results demonstrated that nanoparticles could increase the leaf's ability to absorb solar energy (24.9 %). Dehydrogenase, esterase, acid phosphatase, alkaline phosphatase, and nitrate reductase were among the beneficial enzymes whose functions were considerably improved. This improved native nutrient mobilization by plants and increased uptake of Fe, Cu, Zn, P, and Mg. There was an apparent rise in length, biomass of root and tip count as a result of the use of nano-Mg. The findings indicated that magnesium nanoparticles made through biosynthesis may be used in agriculture to increase crop output [14]. In_2O_3 and AuNPs were synthesized from *A. mexicana* and *Mentha piperita*, respectively, and CuO and Zn NPs from *C. sativa*. These NPs synthesized from Cannabis were then used for foliar application to study its effect on the growth and development of *Glycine max* [15,16].

Plants generate a wide variety of secondary metabolites that are useful in the creation of pharmaceutical medications because they act as defense mechanisms against biotic and abiotic stresses and as remedies for a number of human ailments. Research has assessed numerous compounds with antibacterial, antitumor, anti-inflammatory, and antioxidative properties, as well as their modes of action and possible uses in pharmacology and medicine [17]. Size, shape, and other characteristics of SnO_2 NPs were altered during the biogenic production process utilizing diverse plant species and plant parts [18]. Cerium oxide nanoparticles, or CeO_2 NPs, are used in a variety of applications, including photocatalysis, cancer therapy, and sensors. The green synthesis of CeO_2 NPs is achieved by the use of phytochemicals derived from plant extracts, which adhere to the NPs and function as reducing and/or oxidizing agents, capping agents to stabilize them, and modify the size, morphology, and band gap energy of the NPs [19]. ZnO nanoparticles are well known for their stability, versatility, affordability, and ease of use. There have been reports on the effects of biogenic and phytogenic produced zinc oxide nanoparticles on its characteristics and potential processing methods. Since, plants contain biomolecules that can act as capping, oxidizing and reducing agents that speed up the reaction and stabilize the Nps, many plant extract-based methods for ZnO NPs synthesis have been reported [20]. The impacts of plant extract on the physical, chemical, and optical properties of green synthesized ZnO, SnO_2 and CeO_2 NPs were explored, along with a number of plant extraction methods, synthesis methods, and characterization techniques. The impacts of multiples factors on the size, structure and optical band gap energy of metal oxide have been investigated. The size and shape of the produced ZnO, SnO_2, and CeO_2 NPs were found to be influenced by the phytochemicals contained in the extract composition. According to reports, different plants have different extraction processes depending on the type of plant, plant parts, and solvent utilized [21]. Using the green synthesis approach, pure ZnO NPs and gold decorated (Au-ZnO) hetero nanostructures were created. The reducing agent used in the process was extract from the leaves of peanut (*Carya illinoinensis*). The production of the hetero-structure was validated and confirmed by XRD, FTIR, SEM, EDX, HRTEM, and UV–vis analysis. RhB dye was degraded under UV light irradiation in an aqueous solution to test its photocatalytic activity. Au-ZnO provided superior results than ZnO NPs, with a maximum degradation of 95 % achieved in 180 min at basic pH [22].

The Cannabis genus contains approximately 400 secondary metabolites, among which more than 60 are categorized as cannabinoid compounds, *C. sativa* is valued for its quick growth, which makes it a desirable plant for industrial purposes. It's uses include manufacturing of textiles, paper, rope, biofuel, biodegradable plastics, insulating materials, paints, as well as animal feed, due to the low yet irregular lignin content and abundance of bast fibers. In recent years, *C. sativa* has grown in popularity as a medicinal plant with the potential to cure a variety of conditions, including anorexia, cancer, osteoporosis, emesis, multiple sclerosis, pain management, cancer, and inflammation. Neurological conditions like Tourette's syndrome, Huntington's disease, Alzheimer's disease, and Parkinson's disease have been reportedly treated by Cannabis derived compounds. The biologically active compounds of hemp include cannabinol, Δ-9-THC and cannabidiol (CBD) etc. Notably, CBD, is a prominent non-psychoactive, phytocannabinoid innate to the Cannabis plant and a member of the Cannabaceae family. CBD is structurally a 21-carbon terpenophenolic chemical, which belongs to a category of compounds known for their aromatic rings that contain one or more hydroxyl groups. Researchers use this property to manage the creation of nanoparticles and it is dependent on the presence of these hydroxyl groups for their bio reduction capabilities. It has been shown that phenolic compounds, like those found in CBD, contribute to the stabilization of nanoparticles by establishing interactions with metal atoms that increase their stability when compared to other reducing agents. This occurrence highlights the versatility of nanoparticles with phenolic compound caps. The leaves of hemp plants are often thought of as byproducts as they are mainly grown for their seeds. These leaves, which come from cultivars producing more oil from seed, are the focus of this study.

The objective is to isolate biomolecules and explore their potential to aid in the environmentally friendly manufacturing of nanoparticles. Scientists have synthesized nanoparticles eg., silver nanoparticles (AgNPs) using *C. sativa* leaf extracts, creating unique

materials with a range of medicinal and environmental benefits. To create more potent treatments for bacterial biofilms, their investigations combined the intrinsic antibacterial activity of AgNPs with this medicinal plant [23–25]. Gold nanoparticles (AuNPs) synthesized by the use of *C. sativa* were tested for their therapeutic potential and results showed that they can efficiently be used for biomedical applications. In a different study [26], used Cannabis leaf extracts to produce environment-friendly ZnO NPs. The effectiveness of these nanoparticles as antioxidant and dye-degrading agents was evaluated. The work showed that ZnO NPs could be successfully synthesized from Cannabis leaf extracts and highlighted their potential for use in antioxidant-based therapeutics and wastewater remediation [27]. There is no report to date of the synthesis of SNPs using Cannabis leaf extract. This work demonstrates a novel biogenic manufacturing of sulphur nanoparticles, hence extending the spectrum of beneficial applications of this multifunctional plant owing to its huge and diverse range of secondary metabolites. The results of these studies taken together demonstrate the potential of using Cannabis leaf extracts for the synthesis of nanoparticles with a variety of applications in the biomedical, environmental, and agricultural sectors and contribute to the growing field of nanobiotechnology [23,24,28,29]. Sulphur, a non-toxic and harmless non-metal, is renowned for its antimicrobial properties and capability to form organosulfur compounds in plant tissues. Consequently, sulphur nanomaterials have garnered interest for use in nanomedicines, implants, and medical devices [28–31]. Additionally, sulphur is frequently used as a pesticide in agricultural fields to combat various plant diseases, including powdery mildews, rust, smut fungi, and *Fusarium oxysporum*, which directly affects the growth of Cannabis. While nanomaterials have shown potential in enhancing plant growth, their effects on fruit quality and nutritional elements remain relatively unexplored. Studies have examined the impacts of nanomaterials such as CeO_2, CuO, ZnO, FeO, and ZnFeCu-oxide on plant growth and development processes through foliar spray applications, showcasing their feasibility in directed substance delivery into plant cells [27,32–34]. In pursuit of precision farming, which aims to increase crop yield while, minimizing the use of pesticides and fertilizers, the development of affordable, eco-friendly nano-fertilizers has become imperative [32,33]. The current study is based on the green chemistry theory, and explains the application of safe, ecofriendly methods to reduce the adverse impacts of chemical production on the environment and human health. Plants are employed more effectively for the production of nanoparticles in many cases of biological nanoparticle synthesis because they play a significant role in precursor reduction [34]. According to several studies, plant-derived nanoparticles, particularly those made from leaf extract, are more stable than those made from other biological systems. Alkaloids, polysaccharides, flavonoids, terpenoids, and other biomolecules may play a role in bio-reduction and stabilization of nanoparticles [34]. In our study the production of a unique biogenic nanomaterial that can exhibit dual functions as a plant growth promoter and an effective antibacterial agent has been done. According to our investigation, this nanomaterial, made up of sulphur nanoparticles synthesized from naturally growing Cannabis leaf extract, has a lot of significance for use in agriculture since it has great water-holding ability, which enables it to hold moisture in the soil. Additionally, sulphur in the nanomaterial addresses the problem of leaching frequently associated with commercial fertilizers by allowing the meticulous release of nutrients into the soil. By producing reactive oxygen species, the sulphur component also improves antibacterial action thus, it is a powerful sterilizer against pathogenic bacteria [35]. Biologically active substances such as cannabinoids, terpenes, and phenolic compounds, which have antibacterial, antifungal, anti-inflammatory, and anticancer activities, are found in *C. sativa* (Hemp). To increase the use of *C. sativa* as a support tool in the sector of bio-nanotechnology, we investigated the plant for a green and an effective method of producing sulphur nanoparticles. We have seen its growth-promoting activity in Cannabis plants in a 30-day pot experiment by foliar application of this nanomaterial. This study is significant since it is the first to examine the use of green-synthesized sulphur in agriculture and shows how effective it can be. Our research offers an approach to the development of low-cost nano-fertilizer to sustainable agriculture practices. This research represents a significant achievement because it is the first of its type to show how green sulphur nanoparticles effectively kill human, and fish pathogenic bacteria and at the same time promote plant growth and development.

2. Materials and methods

Analytical grade Chemicals like sodium thiosulfate pentahydrate ($Na_2S_2O_35H_2O$) and HCl were obtained from Sigma-Aldrich, India. Microorganisms such as *S. aureus* (MTCC441), *E. coli* (MTCC443), *A. salmonicida* (MTCC1522), *K. pneumoniae* (MTCC3384) were obtained from the Department of Biotechnology, Sir J. C. Bose Technical Campus, Bhimtal, Kumaun University Nainital, India. All the other analytical and molecular biology grade chemicals were purchased from Himedia, India. *C. sativa* leaves were collected from naturally growing Cannabis plants of Kumaun Himalayas of Uttarakhand, India for SNP synthesis. Seeds were also collected from the same region for plant growth studies. We have obtained a Licence for doing research on *C. sativa* from the Government of Uttarakhand, India.

2.1. Aqueous extract preparation of C. sativa leaves

The extract was prepared according to Ref. [36], with slight modifications. Cannabis leaves were properly cleaned with running water. They were then dried at 60 °C overnight. By using liquid nitrogen, sterile leaves were ground into a fine powder. 500 ml of DDW and 20 g of dried *C. sativa* leaf powder were combined, and the mixture was then incubated for 8 h at 70 °C in a water bath before being filtered through filter paper. The filtrate was stored in a refrigerator at 4 °C for further use.

2.2. Synthesis of sulphur nanoparticles (SNPs)

For the synthesis of SNPs, the method of [37] was used. 24.8 g of $Na_2S_2O_35H_2O$ was added and diluted with 500 ml of *C. sativa* leaf extract followed by gradually adding 10 % HCl dropwise with gentle stirring to allow for consistent sulphur precipitation. SNPs were

produced during synthesis as observed by changes in the color of the reaction mixture. The brownish sodium thiosulfate pentahydrate solution changed to a turbid, yellowish color once SNPs were formed (Suppl. Fig. S1). Resultant suspended sulphur particles were subsequently spun at 5000 rpm at RT for 10 min. For the removal of biological elements, the precipitate was continuously washed with DDW and 100 % EtOH, and the supernatant was discarded. Finally, the product was dried in hot air oven for 4 h at 60 °C and yellow powder was stored for further use (Inset Fig. 4).

2.3. Characterization of sulphur nanoparticles

To verify the synthesis of SNPs (Evolution™260 Bio UV–visible, Thermo Fisher Scientific) in the range of 200–800 nm, the biologically reduced sulphur nanoparticles were subjected to UV–vis spectrophotometer analysis to validate the synthesis of SNPs (Evolution™260 Bio UV–visible, Thermo Fisher Scientific) in the range of 200–800 nm. FTIR studies were carried out utilizing the VERTEX 70v from Bruker Optics for functional group analysis of the samples in order to identify potential leaf extract biomolecules that were in charge of the ion reduction and capping of nanoparticles. A drop of the sample was cast onto a glass slide, let to air dry, and then examined using an X-ray diffractometer (M. Smartlab, Rigaku) to determine the SNPs' XRD pattern. The spectra were recorded using Cu Kα radiation (wavelength of 0.1541 nm) in the range of $2\theta = 10–80^{\circ}$ diffraction angles. EDX on SEM equipment was used to analyze the elemental composition analysis of SNPs by JEOL JCM 6000 Plus NEOSCOPE tabletop SEM coupled with an energy dispersive x-ray analyzer. 10 μL of sample was poured onto the Cu grid that had been coated in carbon and left to dry. Transmission electron microscope EcnaiG20 HR-TEM operating at 200 kV was used for the SNP size analysis (FEI, Electron Optics).

2.4. Antibacterial activity

The Disc diffusion method (DDM) used to check the antibacterial activity, wherein, various doses of biosynthesized SNPs viz. 8, 12, 16, 20 μL from a stock solution of 15 mg mL^{-1} were tested for their antibacterial activity using four pathogenic strains of bacteria, including gram-positive *S. aureus* (MTCC737) and gram-negative *E. coli* (MTCC443) an aquatic fish pathogenic gram-negative, *A. salmonicid*a (MTCC1522), and *K. pneumoniae* (MTCC3384). Inoculums from freshly revived cultures were incubated in Luria-Bertani agar medium-coated petri plates. After a 24-h incubation period, a loop full of culture was incubated overnight in LB broth. An aliquot (100 μl) of the resulting culture was consistently spread using a glass spreader on the LB plate, and it was then incubated at 37 °C for 24 h. Six 8 mm filter paper discs were air dried, and sterilised using UV lamp for 45 min loaded with 8, 12, 16, and 20 μL of SNPs and were placed on an LB plate on which the strains were initially grown. The agar plates were incubated overnight at 37 °C before the ZOI's diameter was determined. The positive control was the aminoglycoside antibiotic streptomycin sulfate (20 μL), and the negative control was DDW. Triplicates of each experiment were done.

2.5. Foliar applications of SNPs

Cannabis plants were raised in plastic containers with a 1:1:1 mixture of peat, soil, and sand in a fully automated greenhouse situated in our department. Seeds (in triplicates) were sprayed with SNP solutions of various concentrations (0.1–1.2 mg mL^{-1}) concentrations, on day 1 and again on day 14 in May–June 2022. Plants under treatment of SNPs and control (triplicates) were maintained, observed, and uprooted after 30 days, and their root, and shoot lengths (cm); fresh and dry weights were measured and documented. For measuring fresh weight, the whole uprooted plant was washed to remove any dust particles and then cleaned dried by dry tissue paper and weighed immediately. It was then shade-dried for one week and then weighed.

2.6. SEM analysis of cannabis leaf

After the foliar spray was applied and full plant development was observable, the elemental mapping of Cannabis leaves was examined in SEM-EDX, where the accumulation of nanoparticles inside the leaves was visualized. A cross-section of the leaf was placed in a dehumidifier for 15 min and was then subjected to gold sputtering. Bioaccumulation and transit of SNPs were also studied using elemental mapping.

2.7. Chlorophyll estimation

Treated and untreated plant leaves were collected after 30 days of seed germination in July, weighed, and immersed in 2 % (w/v) dimethyl sulfoxide (DMSO) for 4 h without homogenization at RT. Chlorophyll estimation calculations were based on formulae given by Ref. [38] DMSO was used as a reference, and absorbance was measured at 645 and 663 nm.

1. Chlorophyll *a* (mg/g) $= (12.7 * A663) - (2.59 * A645)$ (1)
2. Chlorophyll *b* (mg/g) $= (22.9 * A645) - (4.7 * A663)$ (2)
3. Chlorophyll total (mg/g) $= (8.2 * A663) + (20.2 * A645)$ (3)

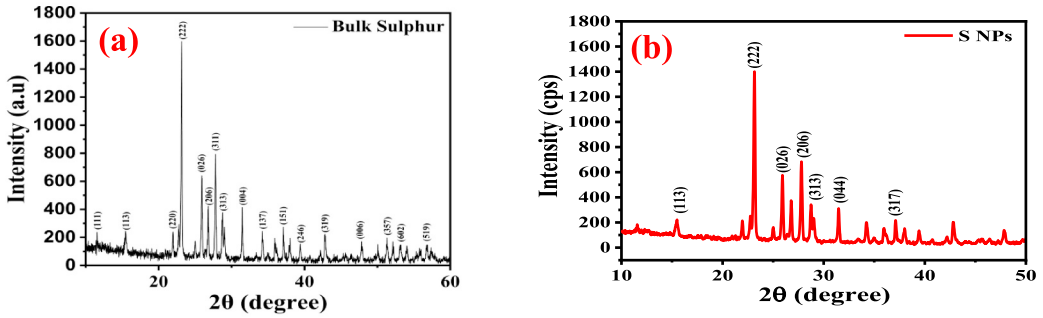

Fig. 1. X-ray diffraction (XRD) pattern of (a) Bulk Sulphur (b) Green synthesized SNPs using Cannabis leaf extract. (For interpretation of the references to color in this figure legend, the reader is referred to the Web version of this article.)

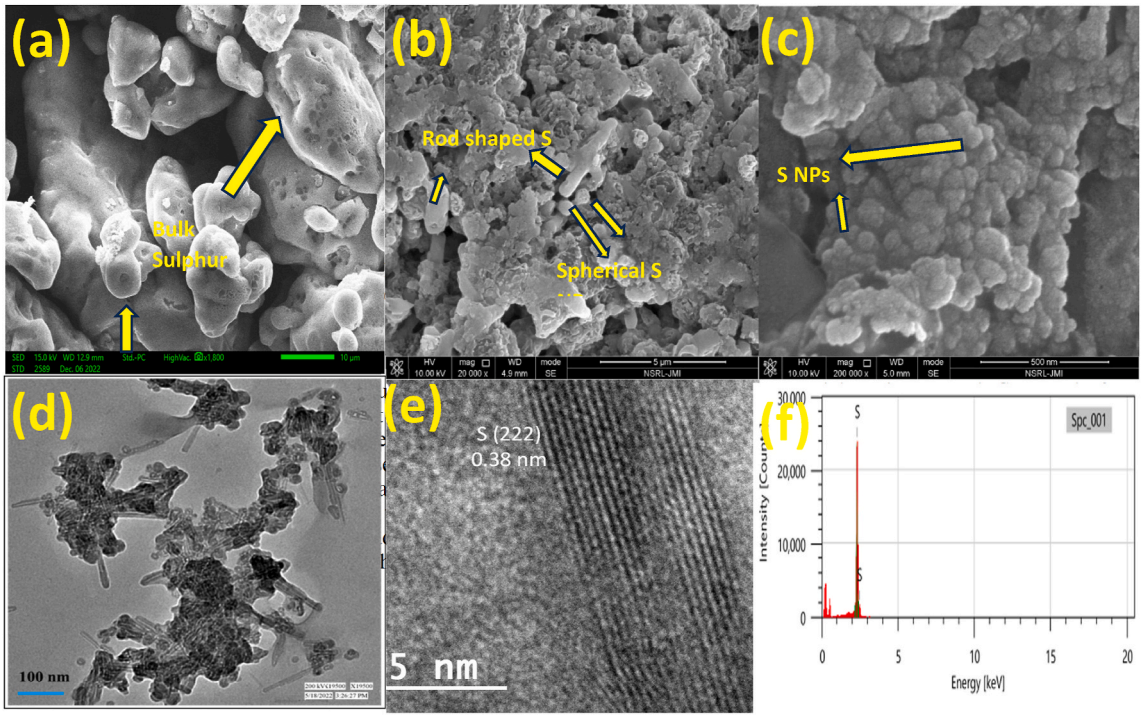

Fig. 2. (a) SEM images showing morphology of bulk Sulphur (b, c) SEM images showing spherical and rod-shaped morphology of synthesized S NPs (d) TEM image of the synthesized sulphur nanoparticles using Cannabis leaf extract, (e) HRTEM image from a portion of the rod-shaped nanoparticles (f) EDAX of the nanoparticles.

3. Results and discussion

3.1. Characterization of SNPs

X-ray diffraction results of the as-synthesized S nanoparticles (0.5, 3.0, and 5.0 wt%) ZnO NPs and pristine ZnO NPs showed 2θ values related to (113), (222), (026), (206), (313), (317) and (044) planes conforming the formation of orthorhombic α-sulphur (Fig. 1), (JCPDS card No: 74–1465) [37] and no other impurity phases are found, showing the good phase purity of SNPs. The presence of highly intense peaks represents the highly crystalline nature of the samples. Moreover, a strong characteristic peak at 23° (222), part of the orthorhombic phase of sulphur is visible in bulk sulphur powder.

Bulk sulphur showed spherical shaped particles with slight agglomeration, and are polydisperse nature (Fig. 2a). TEM images revealed the formation of both nanorods and spherical-shaped particles. Mostly, nanorods having a width of ~20–25 nm and a length of 50–100 nm (Fig. 2) are seen in the image. In addition, some spherical particles of size ~20–30 nm were also formed. HRTEM image of the rod-shaped particles clearly shows the crystal fringe spacing of 0.38 nm which can be indexed to the (222) planes of sulphur

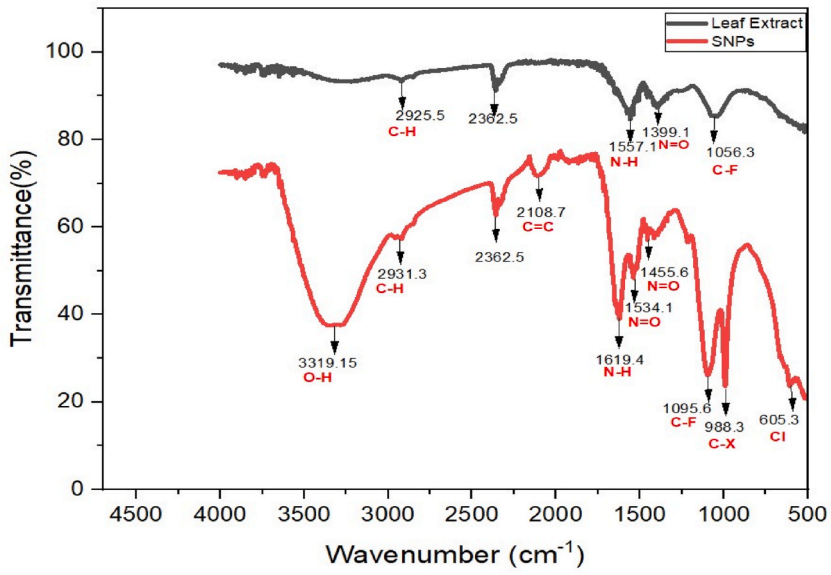

Fig. 3. FTIR spectra of the pure leaf extract and as-synthesized SNPs.

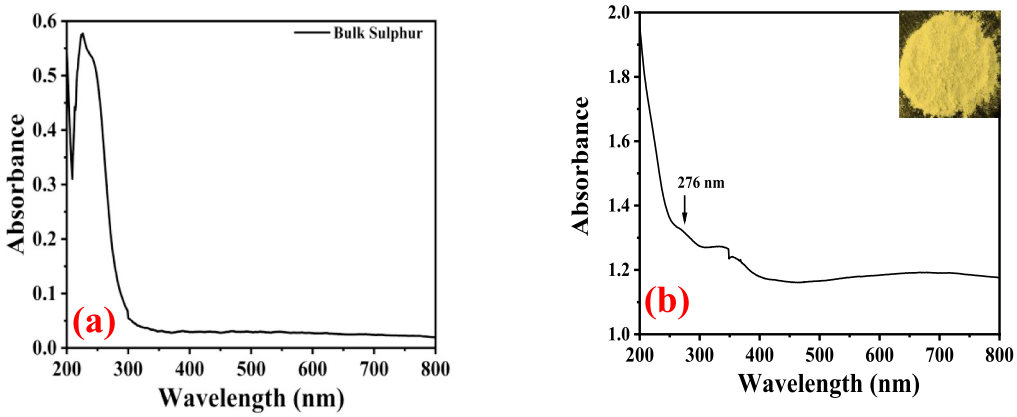

Fig. 4. UV–vis spectra of (a) Bulk Sulphur (b) Green synthesized S NPs using Cannabis leaf extract between 200 and 800 nm showing a peak around 280 nm and thus, confirming green synthesis of S NPs [Inset]. (For interpretation of the references to color in this figure legend, the reader is referred to the Web version of this article.)

nanoparticles. The elemental composition and distribution of the elements can be seen using EDAX, which exposes the X-ray peaks of S that correlate to S nanoparticles, as well as surface topography. It has been noted that sulphur nanoparticles exhibit strong absorption spectra at 280 nm.

Fig. 2 (a) SEM images showing morphology of bulk Sulphur (b, c) SEM images showing spherical and rod-shaped morphology of synthesized S NPs (d) TEM image of the synthesized sulphur nanoparticles using Cannabis leaf extract, (e) HRTEM image from a portion of the rod-shaped particles (f) EDAX of the particles.

The FTIR spectra are used to study the functional group analysis of the synthesized nanoparticles (Fig. 3). Both *C. sativa* leaf extract and SNPs showed a broad peak at ~3200–3400 cm −1 due to –OH and/or –NH stretching vibrations, whereas, the peaks arrived at 2930 and 2855 cm −1 may be due to C-H stretches. Both the spectra reveal intense peaks at 2358 cm −1 for the O=C=O bond vibrations. The peaks present in pure leaf extract at ~1570, 1393, and 1050 cm −1, can be assigned to C=O, C-N, and C-O (of alcohol) stretching vibrations, respectively. The slight shifting of the aforementioned peaks in the SNPs as compared to the pure extract is visible in the spectra. This can be correlated to the interaction of the synthesized SNPs with the biomolecules present in the extract. In addition to the peaks of extract, SNPs display additional peaks at 610, 667, 990, and 1540 cm −1, which can be attributed to the presence of S8.

UV–vis spectral investigations were conducted to measure the nanoparticles' absorption peak. According to Refs. [40,42,43]

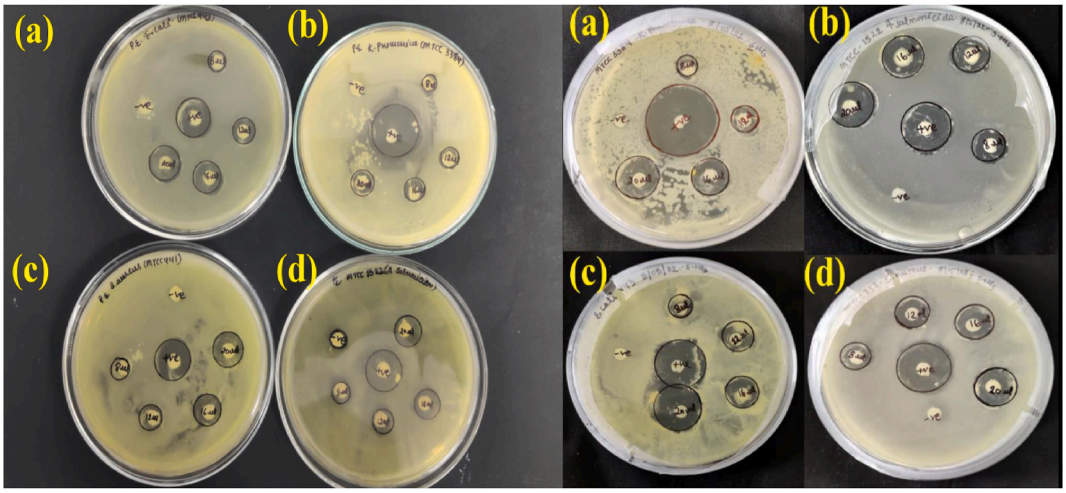

Fig. 5. Antibacterial activity: (a) only *C. sativa* leaf extract application (b) biologically synthesized sulphur nanoparticles (S NPs) against gram-negative *E. coli* (MTCC443), *K. pneumoniae* (MTCC3384), *A. salmonicida* (MTCC1522) and gram-positive *S. aureus* (MTCC737). The ZOI have been shown in Table 1.

synthesized SNPs showed a peak at about 280 nm (Fig. 4), indicating the production of S NPs from *C. sativa* leaf extract. The shift from state b2 to e3 is represented by a secondary peak at 354 nm. Additionally, it was noted that from 400 to 800 nm a slight hump was visible, confirming that these SNPs can be used for visible region photocatalysis for the removal of pollutants from wastewater.

3.2. Mechanism of formation of S NPs

In the treatment of leaves extracts of *C. sativa* with sodium thiosulfate pentahydrate ($Na_2S_2O_35H_2O$) and acidic solution (HCL) (1), a yellowish precipitate appeared in the solution, indicating the synthesis of sulphur nanoparticles (2). According to the following equation, $Na_2S_2O_3$ undergoes a disproportionation reaction to produce S and H_2SO_3 in an acidic solution:

$$Na_2S_2O_3 + 2HCl \rightarrow 2NaCl + SO_2 + S\downarrow + H_2O \quad (1)$$

$$SO_2 + H_2O \rightarrow H_2SO_3 \quad (2)$$

3.3. Antibacterial activity

The *in vitro* antibacterial studies by Disc diffusion method shows (Fig. 5) that SNPs exhibited amazing antibacterial property against gram-positive *S. aureus* (MTCC737), and gram-negative *E. coli* (MTCC443), *A. salmonicida* (MTCC1522) an aquatic fish pathogen and *K. pneumoniae* (MTCC3384) bacteria.

In the case of *E. coli* ZOI for 8, 12, 16, and 20 μl SNPs application were found to be 11.6 ± 0.08, 15.0 ± 0.11, 15.2 ± 0.10, and 21.5 ± 0.12 mm, respectively; in case of *K. pneumoniae* ZOI was found to be 10.5 ± 0.12, 11.6 ± 0.05, 15.2 ± 0.20 and 17.8 ± 0.10 mm, respectively. ZOI for *S. aureus* was 13.5 ± 0.11, 15.0 ± 0.20, 17.0 ± 0.33, and 18 ± 0.12, respectively, for above-mentioned concentrations of SNPs. In case of *A. salmonicida* ZOI,13.5 ± 0.04, 15.0 ± 0.09, 17.8 ± 0.10, and 19.1 ± 0.12 mm was recorded. ZOI for 20 μL positive control streptomycin sulfate was found to be 23 ± 0.20, 28 ± 0.05, 23 ± 0.05, and 20.5 ± 0.05 mm for *E. coli, K. pneumoniae, S. aureus* and *A. salmonicida*, respectively (Table 1).

For the microorganisms in the negative control (deionized water), there was no ZOI seen. However, elemental sulphur did not exhibit any antibacterial effect against four bacteria, and only *C. sativa* leaf extract application was shown to have poor antibacterial activity. The potential of biologically created sulphur nanoparticles (gSNPs) against Gram-positive and Gram-negative bacteria was afterwards substantiated by the study's findings. Sulphur has been utilized for medical purposes since ancient times and has been shown in prior studies to possess antibacterial effects [39]. According to several studies [40–42]. The antibacterial activity of SNPs may be primarily due to the fact that they stop nutrients from entering the cell, break down the bacterial cell walls, and/or block ion transport channels, ultimately leading to cell death, The second likely mechanism is that nanoparticles attach to the ribosome and obstruct cellular translation. Additionally, there is a chance that they will connect to the DNA and break it, which would ultimately result in cell death [43].

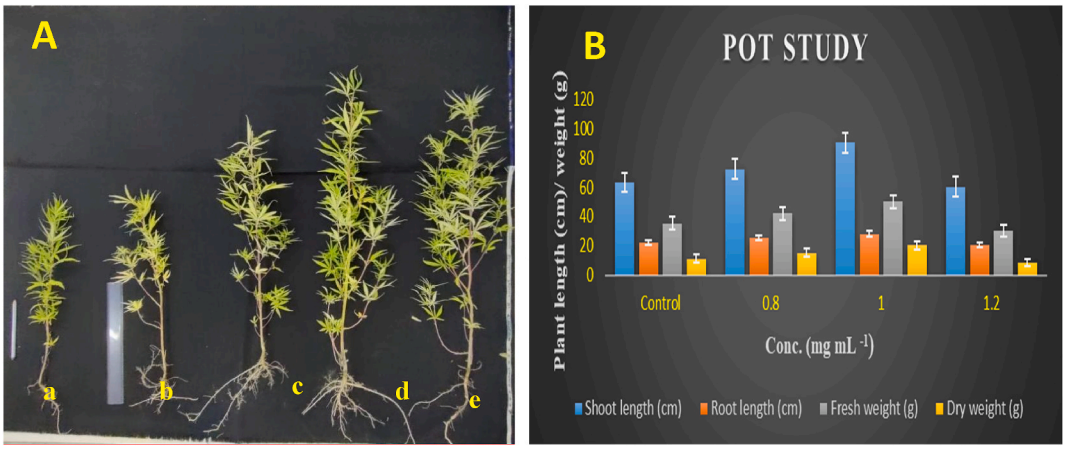

Fig. 6. A. Shoot and root length measurement of uprooted 30 days old Cannabis plants treated with S NPs **a.** 0.2 mg/ml **b** 0.4 mg ml^{-1} **c** 0.8 mg/ml **d** 1.0 mg ml^{-1} **e**. Control. **B.** Bar diagram showing effect of foliar spray of green synthesized S NPs using Cannabis leaf extract on Cannabis plants shoot, root length and fresh, dry weight after 30 days of treatment in pot experiments are also displayed in Table 2. (For interpretation of the references to color in this figure legend, the reader is referred to the Web version of this article.)

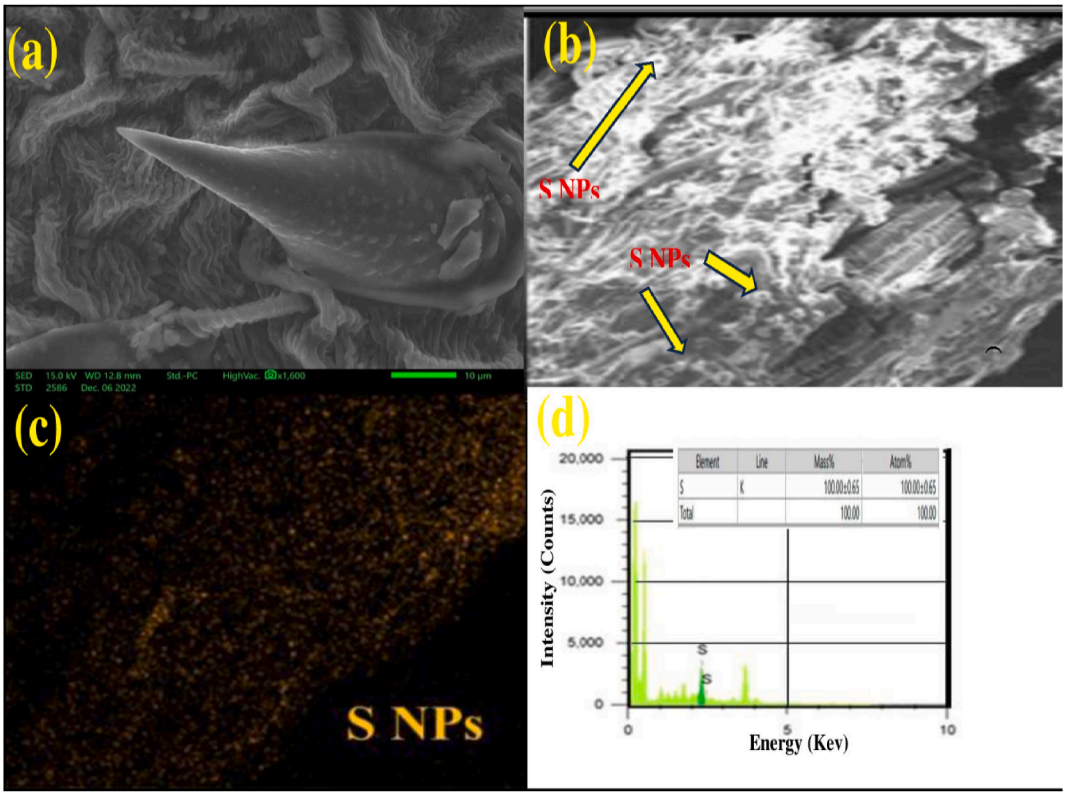

Fig. 7. Elemental mapping of cross section of Cannabis leaf showing (a) control (no nano fertilizer) (b–d) deposition of green synthesized SNPs on the veins of leaf through SEM-energy dispersive X-ray spectrum (SEM-EDX) studies showing the presence of S elements and plant extract elements on leaf. (For interpretation of the references to color in this figure legend, the reader is referred to the Web version of this article.)

3.4. Foliar applications of S NPs

A greenhouse experiment was done to examine the effects of S NP foliar spraying on the growth of Cannabis. Results demonstrated that after 30 days Cannabis plants treated with 1.0 mg ml^{-1} S NPs recorded highest increase in shoot length (90 cm) with thick shoot and increased root length (28 cm) with highest fresh and dry weight (50 g and 20 g, respectively) with greener and healthy leaves, at

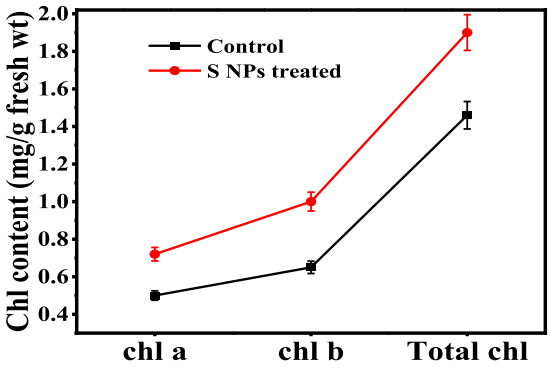

Fig. 8. Chlorophyll estimation of SNPs treated and untreated cannabis plant.

Table 1
Zone of inhibition (ZOI) of SNPs against bacterial strain of *E. coli* (MTCC 443), *S. aureus* (MTCC 441), *K. pneumoniae* (MTCC 3384), *A. salmonicida* (MTCC 1522).

Bacterial strain	Concentration (Volume in μL) stock (15 mg mL^{-1})	Zone of inhibition (diameter in mm)	Zone of inhibition (diameter in mm)
***E. coli* (MTCC443)**		**SNPs**	**Streptomycin sulfate**
	8	11.6 ± 0.08	
	12	15.0 ± 0.11	
	16	15.2 ± 0.10	
	20	21.5 ± 0.12	23 ± 0.20
***S. aureus* (MTCC441)**			
	8	13.5 ± 0.11	
	12	15.0 ± 0.20	
	16	17.0 ± 0.33	
	20	18.0 ± 0.12	23 ± 0.05
***K. pneumoniae* (MTCC 3384)**			
	8	10.5 ± 0.12	
	12	11.6 ± 0.05	
	16	15.2 ± 0.20	
	20	17.8 ± 0.10	28 ± 0.05
***A. salmonicida* (MTCC 1522)**			
	8	13.5 ± 0.04	
	12	15.0 ± 0.09	
	16	17.8 ± 0.10	
	20	19.1 ± 0.12	20.5 ± 0.05

Table 2
Plant growth studies in pot experiments after 30 days of treatment with S NPs. Foliar spray of S NPs was done on the first day of seed sowing and on 14th day of experiment.

Material	Shoot length (cm)	Root length (cm)	Fresh weight (g)	Dry weight (g)
Control	63 ± 0.18	22 ± 0.24	35 ± 0.16	11 ± 0.21
0.1 mg mL^{-1}	39 ± 0.13	17 ± 0.15	22 ± 0.13	6.0 ± 0.23
0.2 mg mL^{-1}	43 ± 0.22	19 ± 0.19	25 ± 0.18	9.0 ± 0.26
0.4 mg mL^{-1}	50 ± 0.12	23 ± 0.56	29 ± 0.14	10.0 ± 0.29
0.8 mg mL^{-1}	72 ± 0.33	25 ± 0.13	42 ± 0.09	15.0 ± 0.31
1.0 mg mL^{-1}	90 ± 0.22	28 ± 0.19	50 ± 0.18	20.0 ± 0.26
1.2 mg mL^{-1}	60 ± 0.12	20 ± 0.56	30 ± 0.14	8.0 ± 0.29

*Mean value SD were used to depict the values in the table.

0.8 mg mL^{-1} S NPs application 72 and 25 cm of shoot and root length, respectively, was recorded with fresh and dry weight of 42 g and 15 g, respectively, while with 1.2 mg ml^{-1} SNPs treatment showed a decrease in both the growth parameters as compared to control (shoot/root length, 60/20 cm; fresh/dry weight, 30/8 g) whereas, untreated plant had shoot and root length of 63 and 22 cm, respectively, with 35 and 11 g fresh and dry weight (Fig. 6).

Treatments lower than 0.8 mg mL^{-1} didn't show significantly better growth as compared to control and 1.2 mg ml^{-1} SNPs treatment showed a decrease in biomass as compared to control which could be due to toxicity induced by higher concentration of

nanomaterial (Table 2) [44]. These findings may be further validated in field experiments also. Gold NPs showed toxic effect above 100 mg/L concentrations and size less than 5 nm, still the underlying mechanism isn't still understood. Toxicity studies of NPs have been done majorly on animals and bacteria, and very less in plants [45].

Considering the collection and effect of nanoparticles on the surface of plant leaves, after the 30th day of foliar spray of nanoparticles, a few fresh leaves were taken, and their cross-section was observed under SEM-EDX for mapping. In SEM images nanoparticle morphology was not visible but the elemental mapping revealed the deposition of SNPs on the surface of leaves (Fig. 7). Further, the thick shoot and better shoot length prove that the nanoparticles were transported from leaves to shoot [4].

3.5. Chlorophyll (chl) estimation

Fig. 8 reveals that the treated plants had higher chl content than the control. High values of chl a, chl b and Total chl could be due to lower stress levels in plants which is associated with high shoot, and root length hence better growth rate [2].

4. Conclusion

According to our knowledge, this is the first account of an easy, affordable, environmentally friendly, and competent enough procedure for preparing green synthesized SNPs by using Cannabis plant extract with high yield as compared to other technologies and methods. Sulphur nanoparticles' effective antibacterial efficacy against the bacteria *E. coli*, *S. aureus*, *A. salmonicida* (a fish pathogen), and *K. pneumoniae* was demonstrated in a study. According to the results of UV–VIS Spectroscopy, SEM, TEM, HRTEM, and FTIR investigations, gSNPs had an average size of 20 nm and a spherical form. Phytochemicals like cannabinoids, phenols, flavonoids, and amino acids were also found on the nanoparticle surface and served as reducing and capping agents. As evidenced by the release of carbohydrates, proteins, and nuclear material via damaged membranes, nanoparticles prevented bacterial growth and changed the permeability of the membrane. It has been reported that SNPs have positive impact on plant growth and development by sustained release of sulphur, an important macronutrient of plants, additionally it has known to improve both biotic and abiotic stress tolerance along with plant metabolism. Cannabis plant growth studies have demonstrated that nanoparticles act as fertilizer for plants. 1 mg mL^{-1} SNPs foliar spray on plants showed a 30 % increase in biomass-enhanced shoot thickness, shoot/root length with high fresh/dry weight and high chl content as compared to control and no toxicity at low concentrations of SNPs proved to be a potent plant growth promoter. After extensive animal testing, this material may also be employed to address medication resistance issues and to modify the genetic makeup of cannabis in order to enhance its therapeutic benefits.

Data availability statement

All data generated or analysed during this study are included in this article.

Ethics approval

Not applicable.

Funding

This research received no external funding.

CRediT authorship contribution statement

Khushboo Dasauni: Writing – original draft, Investigation, Conceptualization. **Tapan K. Nailwal:** Writing – review & editing, Supervision, Project administration. **Bhavani Prasad Naik Nenavathu:** Supervision.

Declaration of competing interest

The authors declare that they have no known competing financial interests or personal relationships that could have appeared to influence the work reported in this paper.

Acknowledgments

The authors are grateful to Kumaun University Nainital, Uttarakhand for providing infrastructure and for necessary instrumentation facilities.

Appendix A. Supplementary data

Supplementary data to this article can be found online at https://doi.org/10.1016/j.heliyon.2024.e37797.

References

[1] R. Mohammadinejad, S. Karimi, S. Iravani, R.S. Varma, Plant-derived nanostructures: types and applications, Green Chem. 18 (1) (2016) 20–52, https://doi.org/10.1039/C5GC01403D.

[2] F. Kang, P.J. Alvarez, D. Zhu, Microbial extracellular polymeric substances reduce Ag^{+} to silver nanoparticles and antagonize bactericidal activity, Environ. Sci. Technol. 48 (1) (2014) 316–322, https://doi.org/10.1021/es403796x.

[3] R. Singh, U.U. Shedbalkar, S.A. Wadhwani, B.A. Chopade, Bacteriagenic silver nanoparticles: synthesis, mechanism, and applications, Appl. Microbiol. Biotechnol. 99 (2015) 4579–4593, https://doi.org/10.1007/s00253-015-6622-1.

[4] D.P. Yang, S. Chen, P. Huang, X. Wang, W. Jiang, O. Pandoli, D. Cui, Bacteria-template synthesized silver microspheres with hollow and porous structures as excellent SERS substrate, Green Chem. 12 (11) (2010) 2038–2042, https://doi.org/10.1039/c0gc00431f.

[5] V. Bansal, D. Rautaray, A. Ahmad, M. Sastry, Biosynthesis of zirconia nanoparticles using the fungus Fusarium oxysporum, J. of Mater. Chemistry 14 (22) (2004) 3303–3305, https://doi.org/10.1039/B407904C.

[6] A. Syed, A. Ahmad, Extracellular biosynthesis of platinum nanoparticles using the fungus Fusarium oxysporum, Colloids Surf., B 97 (2012) 27–31, https://doi.org/10.1016/j.colsurfb.2012.03.026.

[7] A.M. Mansour, B.A. Hemdan, A. Elzwawy, A.B. Abou Hammad, A.M. El Nahrawy, Ecofriendly synthesis and characterization of Ni^{2+} codoped silica magnesium zirconium copper nanoceramics for wastewater treatment applications, Sci. Rep. 12 (1) (2022) 9855, https://doi.org/10.1038/s41598-022-13785-y.

[8] H. Bahrulolum, S. Nooraei, N. Javanshir, H. Tarrahimofrad, V.S. Mirbagheri, A.J. Easton, G. Ahmadian, Green synthesis of metal nanoparticles using microorganisms and their application in the agrifood sector, J. Nanobiotechnology. 19 (1) (2021) 1–26, https://doi.org/10.1186/s12951-021-00834-3.

[9] A.K. Mittal, Y. Chisti, U.C. Banerjee, Synthesis of metallic nanoparticles using plant extracts, Biotechnol. Adv. 31 (2) (2013) 346–356, https://doi.org/10.1016/j.biotechadv.2013.01.003.

[10] A. Yan, Z. Chen, Impacts of silver nanoparticles on plants: a focus on the phytotoxicity and underlying mechanism, Int. J. Mol. Sci. 20 (5) (2019) 1003, https://doi.org/10.3390/ijms20051003.

[11] C. Larue, H. Castillo-Michel, S. Sobanska, L. Cécillon, S. Bureau, V. Barthès, L. Ouerdane, M. Carrière, G. Sarret, Foliar exposure of the crop Lactuca sativa to silver nanoparticles: evidence for internalization and changes in Ag speciation, J. Hazard Mater. 264 (2014) 98–106, https://doi.org/10.1016/j.jhazmat.2013.10.053.

[12] J.Y. Cheon, S.J. Kim, Y.H. Rhee, O.H. Kwon, W.H. Park, Shape-dependent antimicrobial activities of silver nanoparticles, Int. J. Nanomed. (2019) 2773–2780, https://doi.org/10.2147/IJN.S196472.

[13] R. Krishnasamy, J.M. Obbineni, Methods for green synthesis of metallic nanoparticles using plant extracts and their biological applications-A review, J. Biomim. Biomater. Biomed. Eng. 56 (2022) 75–151, https://doi.org/10.4028/p-8bf786.

[14] I. Rathore, J.C. Tarafdar, Perspectives of biosynthesized magnesium nanoparticles in foliar application of wheat plant, J. Bionanosci. 9 (3) (2015) 209–214, https://doi.org/10.1166/jbns.2015.1296.

[15] P. Kuppusamy, M.M. Yusoff, G.P. Maniam, N. Govindan, Biosynthesis of metallic nanoparticles using plant derivatives and their new avenues in pharmacological applications–An updated report, Saudi Pharmaceut. J. 24 (4) (2016) 473–484, https://doi.org/10.1016/j.jsps.2014.11.013.

[16] I. Karmous, S. Vaidya, C. Dimkpa, N. Zuverza-Mena, W. da Silva, K.A. Barroso, J. Milagres, A. Bharadwaj, W. Abdelraheem, J.C. White, W.H. Elmer, Biologically synthesized zinc and copper oxide nanoparticles using Cannabis sativa L. enhance soybean (Glycine max) defense against fusarium virguliforme, Pesticide. Biochem. Physiol (2023) 105486, https://doi.org/10.1016/j.pestbp.2023.105486.

[17] B. Hilal, M.M. Khan, Q. Fariduddin, Recent advancements in deciphering the therapeutic properties of plant secondary metabolites: phenolics, terpenes, and alkaloids, Plant Physiol. Biochem. (2024) 108674, https://doi.org/10.1016/j.plaphy.2024.108674.

[18] S. Matussin, M.H. Harunsani, A.L. Tan, M.M. Khan, Plant-extract-mediated SnO_2 nanoparticles: synthesis and applications, ACS Sustain. Chem. Eng. 8 (8) (2020) 3040–3054, https://doi.org/10.1021/acssuschemeng.9b06398.

[19] S.N. Naidi, M.H. Harunsani, A.L. Tan, M.M. Khan, Green-synthesized CeO_2 nanoparticles for photocatalytic, antimicrobial, antioxidant and cytotoxicity activities, J. Mater. Chem. B 9 (28) (2021) 5599–5620, https://doi.org/10.1039/D1TB00248A.

[20] A. Rahman, M.H. Harunsani, A.L. Tan, M.M. Khan, Zinc oxide and zinc oxide-based nanostructures: biogenic and phytogenic synthesis, properties and applications, Bioproc. Biosyst. Eng. 44 (7) (2021) 1333–1372, https://doi.org/10.1007/s00449-022-02713-z.

[21] M.M. Khan, S.N. Matussin, A. Rahman, Recent progress of phytogenic synthesis of ZnO, SnO_2, and CeO_2 nanomaterials, Bioproc. Biosyst. Eng. 45 (4) (2022) 619–645, https://doi.org/10.1016/j.jece.2020.104725.

[22] M. Ahmad, W. Rehman, M.M. Khan, M.T. Qureshi, A. Gul, S. Haq, R. Ullah, A. Rab, F. Menaa, Phytogenic fabrication of ZnO and gold decorated ZnO nanoparticles for photocatalytic degradation of Rhodamine B, J. Environ. Chem. Eng. 9 (1) (2021) 104725, https://doi.org/10.1016/j.jece.2020.104725.

[23] A.C. Csakvari, C. Moisa, D.G. Radu, L.M. Olariu, A.I. Lupitu, A.O. Panda, G. Pop, D. Chambre, V. Socoliuc, L. Copolovici, D.M. Copolovici, Green synthesis, characterization, and antibacterial properties of silver nanoparticles obtained by using diverse varieties of Cannabis sativa leaf extracts, Molecules 26 (13) (2021) 4041, https://doi.org/10.3390/molecules26134041.

[24] S. Mandal, B.M. Sreekar, H. Roxana, A.O. Mohammad, Q.S. Sheldon, Green Sustain. Chem. 11 (1) (2021), https://doi.org/10.4236/gsc.2021.111004.

[25] N. Aziz, M. Faraz, R. Pandey, M. Shakir, T. Fatma, A. Varma, I. Barman, R. Prasad, Facile algae-derived route to biogenic silver nanoparticles: synthesis, antibacterial, and photocatalytic properties, Langmuir 31 (42) (2015) 11605–11612, https://doi.org/10.1021/acs.langmuir.5b03081.

[26] S. Hameed, S. Ali Shah, J. Iqbal, M. Numan, W. Muhammad, M. Junaid, S. Shah, R. Khurshid, F. Umer, Cannabis sativa-mediated synthesis of gold nanoparticles and their biomedical properties, Bioinspired, Biomim 9 (2) (2020) 95–102, https://doi.org/10.1680/jbibn.19.00023.

[27] M.A. Huq, M.A.I. Apu, M. Ashrafudoulla, M.M. Rahman, M.A.K. Parvez, S.R. Balusamy, S. Akter, M.S. Rahman, Bioactive ZnO nanoparticles: biosynthesis, characterization and potential AntimicrobialApplications, Pharmaceutics 15 (11) (2023) 2634, https://doi.org/10.3390/pharmaceutics15112634.

[28] P. Singh, S. Pandit, J. Garnæs, S. Tunjic, V.R. Mokkapati, A. Sultan, A. Thygesen, A. Mackevica, R.V. Mateiu, A.E. Daugaard, A. Baun, Green synthesis of gold and silver nanoparticles from Cannabis sativa (industrial hemp) and their capacity for biofilm inhibition, Int. J. Nanomed. 3571–3591 (2018), https://doi.org/10.2147/IJN.S157958.

[29] M.J. Hawkesford, Plant responses to sulphur deficiency and the genetic manipulation of sulphate transporters to improve S-utilization efficiency, J. Exp. Bot. 51 (342) (2000) 131–138, https://doi.org/10.1093/jexbot/51.342.131.

[30] S. Kim, R. Kubec, R.A. Musah, Antibacterial and antifungal activity of sulfur-containing compounds from Petiveria alliacea L, J. Ethnopharmacol. 104 (1–2) (2006) 188–192, https://doi.org/10.1016/j.jep.2005.08.072.

[31] A.B. Bakry, M.S. Sadak, M.F. El-Karamany, Effect of humic acid and sulfur on growth, some biochemical constituents, yield and yield attributes of flax grown under newly reclaimed sandy soils, J. Agric. Biol. Sci. 10 (7) (2015) 247–259, https://doi.org/10.7813/2075-4124.2013/5-5/A.17.

[32] M.L. López-Moreno, L.L. Avilés, N.G. Pérez, B.Á. Irizarry, O. Perales, Y. Cedeno-Mattei, F. Román, Effect of cobalt ferrite (CoFe2O4) nanoparticles on the growth and development of Lycopersicon lycopersicum (tomato plants), Sci. Total Environ. 550 (2016) 45–52, https://doi.org/10.1016/j.scitotenv.2016.01.063.

[33] Y. Bao, J. He, K. Song, J. Guo, X. Zhou, S. Liu, Plant-extract-mediated synthesis of metal nanoparticles, J. Chem. 2021 (2021) 1–14, https://doi.org/10.1155/2021/6562687.

[34] N.T.T. Nguyen, L.M. Nguyen, T.T.T. Nguyen, R.K. Liew, D.T.C. Nguyen, T. Van Tran, Recent advances on botanical biosynthesis of nanoparticles for catalytic, water treatment and agricultural applications: a review, Sci. Total Environ. 827 (2022) 154160, https://doi.org/10.1016/j.scitotenv.2022.154160.

[35] S. Iravani, Green synthesis of metal nanoparticles using plants, Green Chem. 13 (10) (2011) 2638–2650, https://doi.org/10.1039/C1GC15386B.

[36] S. Ghotekar, T. Pagar, S. Pansambal, R. Oza, A review on green synthesis of sulfur nanoparticles via plant extract, characterization and its applications, Adv. J. Chem B. 2 (3) (2020) 128–143, https://doi.org/10.22034/ajcb.2020.109501.

[37] M. Ramesh, M. Anbuvannan, G. Viruthagiri, Green synthesis of ZnO nanoparticles using Solanum nigrum leaf extract and their antibacterial activity, Spectrochimica Acta Part A: Mol. Biomol. Spectroscopy 136 (2015) 864–870, https://doi.org/10.1016/j.saa.2014.09.105.

[38] N.M. Salem, L.S. Albanna, A.M. Awwad, Green synthesis of sulfur nanoparticles using Punica granatum peels and the effects on the growth of tomato by foliar spray applications, Environ. Nanotechnol. Monit. Manag. 6 (2016) 83–87, https://doi.org/10.1016/j.enmm.2016.06.006.
[39] P. Suryavanshi, R. Pandit, A. Gade, M. Derita, S. Zachino, M. Rai, Colletotrichum sp.-mediated synthesis of sulphur and aluminium oxide nanoparticles and it's in vitro activity against selected food-borne pathogens, LWT–Food Sci. Technol. 81 (2017) 188–194, https://doi.org/10.1016/j.lwt.2017.03.038.
[40] A.K. Gupta, K. Nicol, The use of sulfur in dermatology, J Drugs Dermatol 3 (4) (2004) 427–431.
[41] K. Vijayaraghavan, T. Ashokkumar, Plant-mediated biosynthesis of metallic nanoparticles: a review of literature, factors affecting synthesis, characterization techniques and applications, J. Environ. Chem. Eng. 5 (5) (2017) 4866–4883, https://doi.org/10.1016/j.jece.2017.09.026.
[42] A. Lesniak, A. Salvati, M.J. Santos-Martinez, M.W. Radomski, K.A. Dawson, C. Åberg, Nanoparticle adhesion to the cell membrane and its effect on nanoparticle uptake efficiency, J. American Chem. Soci. 135 (4) (2013) 1438–1444, https://doi.org/10.1021/ja309812z.
[43] A. Singh, K. Dasauni, T. Nailwal, B.P. Nenavathu, TeO2 deposited ZnO nanotubes combined with cefotaxime as a nanoantibiotic against Klebsiella pneumoniae, Mater. Today: Proc. 67 (2022) 451–455, https://doi.org/10.1016/j.matpr.2022.05.350.
[44] M. Rai, A.P. Ingle, P. Paralikar, Sulfur and sulfur nanoparticles as potential antimicrobials: from traditional medicine to nanomedicine. Expert Rev. Anti. Infect, Ther. 14 (10) (2016) 969–978, https://doi.org/10.1080/14787210.2016.1221340.
[45] J. Siegel, K. Záruba, V. Švorčík, K. Kroumanová, L. Burketová, J. Martinec, Round-shape gold nanoparticles: effect of particle size and concentration on Arabidopsis thaliana root growth, Nanoscale Res. Lett. 13 (2018) 1–7, https://doi.org/10.1186/s11671-018-2510-9.